Bubble Size Models for the Prediction of Bubbly Flow with CMFD Code

Jin-yeong Bak , Byong-jo Yun *, Jae-jun Jeong
School of Mechanical Engineering, Pusan National Univ.,
Busandaehak-ro 63 gil, Geumjeong-gu, Busan 609-73, Korea
**Corresponding author: bjyun@pusan.ac.kr*

1. Introduction

In recent years, the use of computational multi-fluid dynamics (CMFD) codes has been extended to the analysis of multi-dimensional two-phase flow for the operation and safety analysis of nuclear power plants (NPP). In these applications, an accurate prediction of bubble behaviors is one of major concerns. Among many two-phase flow parameters, bubble size is a prime important parameter for an accurate prediction of bubble behaviors in the two-phase flow channel. To predict accurately the bubble size distribution in the flowing channel, mechanistic modelling approach such as interfacial area concentration and bubble number density is desirable. Yao and Morel [1] and Yeoh and Tu [2] respectively applied interfacial area concentration transport (IACT) equation and bubble number density transport equation into CMFD code. Recently Lo and Zhang [3] tried to apply the generalized S_γ model to the predictions of not only droplet size in the oil-water flow but also bubble size in the air-water flow.

In this paper, three-dimensional numerical simulations for the gas-liquid two-phase flow were conducted to validate and confirm the performance of S_γ bubble size model for the further application to the narrow rectangular boiling channel for the research reactor core, using the commercial CFD code STAR CCM$^+$ ver. 9.06. For this, S_γ model was evaluated against air-water data of DEDALE [1] and Hibiki et al.'s [4] experiment. These experimental data were obtained in a vertically arranged pipe under upwards air-water flow condition. Detailed descriptions on the S_γ with its breakup and coalescence model are presented in the present manuscript. Additionally, correlation for prediction of the local bubble size was developed by using numerical results that are calculated from DEDALE and Hibiki et al.'s experimental condition. Developed correlation was based on Yun model [5] designed on the basis of DEBORA that is the subcooled boiling data in high pressure condition.

2. Experimental Data

For evaluation of bubble size models for the CMFD code, numerical simulations were carried out against both DEDALE and Hibiki et al.'s [4] experimental data. The DEDALE experimental data were obtained from Yao and Morel [1]. Both of the data used for the present study were obtained under the vertical upwards air-water flowing conditions.

DEDALE experiments were carried out at EDF (Electricity of France) in 1995 [1]. It was conducted in an adiabatic vertical pipe with upwards air-water bubbly flows under the atmospheric pressure condition. The pipe is 6m long in length and has an inner diameter of 38.1mm. Air is injected at the periphery of the water flow in 80 identical holes with an inner diameter of 0.6mm. Measurements are realized at three different axial location: z/D = 8, 55 and 155.

Hibiki et al.'s experiments were performed vertical pipe of which inner diameter is 50.8mm and the height is 3.06m. Water and air in the atmospheric condition were used as working fluids. Measurements were taken in two axial positions: z/D = 6.0 and 53.5. Hibiki et al. [4] reported that the initial bubble diameter was about 3mm at the pipe inlet.

In the present work, two cases of DEDALE experiments and four cases of Hibiki et al.'s experiments were chosen to validate S_γ model for bubbly flow. Table I and II show the flow condition and measured two-phase flow parameters of the DEDALE and Hibiki et al.'s experiments, respectively.

Table I: Inlet Condition of DEDALE Experiments

Parameter	DEDALE 1101	DEDALE 1103
J_g (m/s)	0.0588	0.1851
J_l (m/s)	0.877	0.877
α	0.048	0.152
a_i (m^{-1})	97	269

Table II: Flow Conditions and Measured Void Fraction of Hibiki et al.'s Experiments (z/D = 53.5)

Case	J_g(m/s)	J_l(m/s)	α
1	0.321	0.986	0.231
2	0.518	5	0.106
3	0.624	2.01	0.228
4	0.471	2.01	0.183

3. Bubble Size Models

In the present study, S_γ mechanistic bubble size model was evaluated against DEDALE and Hibiki et al.'s experimental data. In addition to this, a new local bubble size correlation was proposed and also evaluated.

3.1 S_γ Bubble Size Model

Recently, Lo and Zhang [3] and Yun et al. [6] applied generalized S_γ equations for the prediction of bubble size in the air-water and steam-water flows, respectively. In the present work, the S_γ model was revisited for the prediction of bubble size with more extensive air-water databases.

S_γ is defined as a generalized parameter for the size distribution of bubble/droplet as follows,

$$S_\gamma = nM_\gamma = n\int_0^\infty d^\gamma P(d)d(d) \qquad (1)$$

where n is the number density, M_γ is the γth moment, d is the bubble size. $P(d)$ is the bubble size distribution which is assumed to be a log-normal distribution in the present work.

The zeroth-moment of the distribution is the number density of the bubble, $n = S_0$. The second-moment, S_2, is related to the interfacial area density a_i ($=\pi S_2$) and the third-moment, S_3, is related to the void fraction α ($=\pi S_3/6$). From these relations, the Sauter mean diameter can be calculated as follows

$$d_{sm} = d_{32} = \frac{S_3}{S_2} = \frac{6\alpha}{\pi}\frac{1}{S_2} \qquad (2)$$

By using the definitions, the transport equation for the generalized S_γ is expressed as follows,

$$\frac{\partial S_\gamma}{\partial t} + \nabla\cdot(S_\gamma u_d) = s_{br} + s_{cl} \qquad (3)$$

where u_d is the dispersed phase velocity, s_{br} and s_{cl} are sources terms for breakup and coalescence respectively.

3.1.1 Breakup Model

The breakup source term s_{br} is defined as follows:

$$s_{br} = \int_0^\infty K_{br}(d)\Delta S_\gamma^{br} nP(d)d(d) \qquad (4)$$

where the K_{br} is the breakup rate, ΔS_γ^{br} is the change in S_γ due to a single breakup event of a bubble of size d. The binary breakup of a bubble with equal size fragments is assumed and the breakup rate K_{br} is equal to the reciprocal breakup time τ_{br}. The breakup source term becomes:

$$s_{br} = \int_0^\infty \frac{d^\gamma (2^{\frac{3-\gamma}{3}} - 1)}{\tau_{br}(d)} nP(d)d(d) \qquad (5)$$

Breakup occurs only if the droplet is larger than the critical diameter d_{cr}. Breakup source term is defined as the sum of the sources for viscous and inertial breakup:

$$s_{br} = s_{br,v} + s_{br,i} \qquad (6)$$

Viscous breakup is found in laminar flows and in turbulent flows for bubble smaller than the Kolmogorov length scale L_k defined by,

$$L_k = \left(\nu_c^3/\varepsilon\right)^{1/4} \qquad (7)$$

where ν_c is the continuous phase kinematic viscosity and ε is the continuous phase dissipation rate of turbulent kinetic energy. On the other hand, larger bubbles are considered to break up by inertia breakup mechanism. Fig. 1 shows graphically the breakup regimes

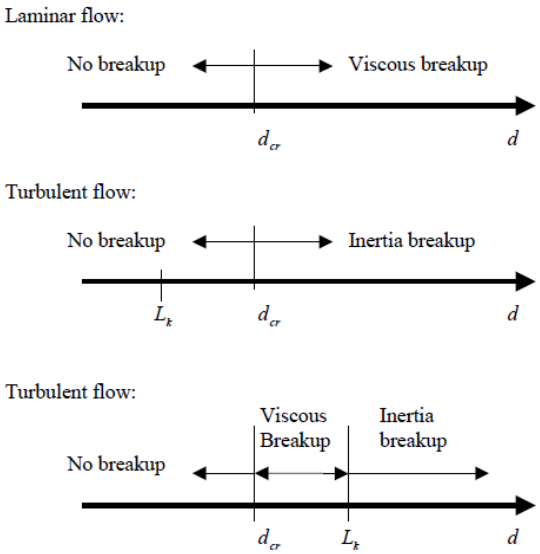

Fig. 1. Breakup Regime of S_γ Model

3.1.2 Coalescence Model

The source term s_{cl} for bubble coalescence in Eq. (3) is given by:

$$s_{cl} = \int_0^\infty \int_0^\infty K_{cl}\Delta S_\gamma^{cl}(d,d')n^2 P(d,d')d(d,d') \qquad (8)$$

where K_{cl} is the coalescence rate of bubble sizes d, d' and $\Delta S_\gamma^{cl}(d,d')$ is change in S_γ due to single coalescence event of bubble size d, d'. From assumption that the volume of bubble is conserve during collision and bubble size has a uniform distribution with an equivalent mean diameter d_{eq}, Eq. (8) becomes,

$$s_{cl} = (2^{\gamma/3} - 2)\left(\frac{6\alpha_d}{\pi}\right)^2 k_{coll} u_{rel} P_{cl}(d_{eq}) d_{eq}^{\gamma-4} \qquad (9)$$

where k_{coll} is the collision rate coefficient, P_{cl} is the coalescence probability of a single collision event and u_{rel} is the typical velocity difference over a range of d_{eq}.

Table III: Summary of Modeling for Breakup Source Term.

Viscous regime
$d_{cr}=\frac{2\sigma\Omega_{cr}}{\mu_c\dot{\gamma}}$, $\Omega=\frac{\mu_c d}{2\sigma}\dot{\gamma}$: capillary number
$\Omega_{cr}=\sqrt{\left(-\frac{c_1}{c_2}(\log\lambda)^2-2\frac{c_4}{c_3}\log\lambda-\frac{1}{c_3}\right)+\left(\frac{c_2}{c_3}\log\lambda+\frac{c_5}{c_3}\right)}-\frac{c_2}{c_3}\log\lambda-\frac{c_5}{c_3}-1$
$\lambda=\mu_d/\mu_c$, c_1 to c_5 : fitting constants
$\dot{\gamma}$: shear rate calculated from local velocity gradient for laminar flow
$\dot{\gamma}=\sqrt{(\varepsilon\rho_c/\mu_c)}$: Kolomogov shear rate for turbulent flow
Breakup occurs when $\Omega \geq \Omega_{cr}$
$\tau_{br}=\frac{\mu_c d}{\sigma}f_\tau(\lambda)$, $f_\tau(\lambda)=p_0+p_1\log(\lambda)+p_2(\log(\lambda))^2$
p_0, p_1, p_2 : empirical constants
Inertial regime
$d_{cr}=\left(1+C_\alpha\alpha_d\right)\left(\frac{2\sigma\Omega_{cr}}{\mu_c\dot{\gamma}}\right)^{3/5}\varepsilon^{-0.4}$
C_α (dispersed concentration factor) = 4.6
$We=\frac{\rho_c u_l^2 d}{\sigma}$, $We_{cr}=0.31$
Breakup occurs when $We \geq We_{cr}$
$\tau_{br}=2\pi k_{br}\sqrt{\frac{(3\rho_d+2\rho_c)}{192\sigma}}$, $k_{br}=0.2$

Table IV: Summary of Modeling for Coalescence Source Term.

Viscous regime
$k_{coll}=(8\pi/3)^{0.5}$, $u_{rel}=\dot{\gamma}d$
$P_{cl}=\exp(-t_d/t_i)$, $t_i=1/\dot{\gamma}$,
$t_d=\frac{\pi\mu_d\sqrt{F_i}}{2h_{cr}}\left(\frac{d_{eq}}{4\pi\sigma}\right)^{1.5}$: partial mobile interface
$F_i=\frac{3\pi}{2}\mu_c\dot{\gamma}d_{eq}^2$: interaction force during the collision
$h_{cr}=\left(\frac{A_H d_{eq}}{24\pi\sigma}\right)^{1/3}$: critical film thickness
$A_H=5\times10^{-21}$: Hamaker constant
Inertial regime
$k_{coll}=(2\pi/15)^{0.5}$, $u_{rel}=(\varepsilon_c d_{eq})^{1/3}$
$P_{cl}=\frac{\Phi_{\max}}{\pi}\left(1-\frac{k_{cl,2}^2(We-We_0)^2}{\Phi_{\max}}\right)^{1/2}$, $\Phi_{\max}=\frac{2h_0^2\rho_c\sigma}{We_0\mu_d^2 d}$, $k_{cl}\approx12.7$
$We_0=0.8We_{cr}$, $h_0=8.3h_{cr}$

Each parameter used breakup and coalescence is modeled according to the viscous and inertial regimes as summarized in Table III and IV ([3] & [6]).

3.2 A New Correlation for the Local Bubble Size

Correlation for the local bubble size was developed based on the Yun model [5]. Yun model is developed by using DEBORA that is subcooled boiling data which is equivalent to high pressure condition of steam-water flow. In the present study, a new correlation is obtained by applying DEBORA, DEDALE and Hibiki et al.'s data to the Yun's correlation as follows,

$$d_{sm}=32.59\alpha^{0.292}N_{\mathrm{Re}b}^{-0.529}N_\rho^{0.06}Lo \qquad (10)$$

where the Reynolds number $N_{\mathrm{Re}b}$, the ratio of density N_ρ, the Laplace length scale Lo is defined as Eq. (11), (12), and (13) respectively.

$$N_{\mathrm{Re}b}=\frac{\varepsilon^{1/3}Lo^{4/3}}{\upsilon_f} \qquad (11)$$

$$N_\rho=\frac{\rho_f}{\rho_g} \qquad (12)$$

$$Lo=\sqrt{\frac{\sigma}{g\Delta\rho}} \qquad (13)$$

4. Numerical Simulation

All the numerical simulations were carried out with the commercial CFD code STAR CCM$^+$ ver 9.06. In the present work, three-dimensional numerical simulations were conducted. The mesh is composed of 20 and 200 cells in the radial and axial directions, respectively, which satisfies y^+ of more than 30 at the first cell node from the wall.

Constitutive models for the interfacial drag, the turbulence models, the wall lift force, the wall lubrication force, etc, are needed for the Eulerian multi-phase flow simulation of bubbly flow. Most of these model have been already implemented into the STAR CCM$^+$ and are selectable by the user. In the present calculation, Troshko and Hassan's [7] particle induced turbulence force model, Antal et al.'s [8] wall lubrication force, Bozzano and Dente's [9] interfacial drag force and constant lift force coefficients are applied. In addition to this, turbulence model is used for continuous phase and dispersed phase. Among these, Wall lubrication force which prevents bubbles from approaching to the wall is important when the many bubbles approach to the wall. Therefore it was applied to only the calculation of DEDALE experimental data which has high local void fraction near the wall as shown Fig. 2.

5. Results and Discussion

The two-phase flow parameters such as void fraction, bubble size and phase velocities predicted with both S_γ model and newly developed bubble size correlation were compared with the experimental data as in the Figs. 2 - 9. The figures show that the numerical results reasonably predict such local two-phase flow parameters.

As shown in Fig. 2, the simulation result for DEDALE 1101 does not capture the decrease of void fraction at the near wall and the core voiding

phenomena regardless of bubble models. The results of S_γ bubble size model in Fig. 3 shows a tendency to over predict the bubble size. Because of these facts, phase velocities have also some discrepancy between the prediction and experimental data as shown in Fig. 4 and 5. In contrast, in the case of DEDALE 1103, the numerical result in Fig. 2 shows that the void fraction distribution is predicted fairly well. Moreover, the numerical results for bubble size and phase velocity predicted well the experimental data as shown in Fig. 3, 4 and 5. The figures show that the new bubble size correlation improves the prediction of bubble size with CMFD code compared to the S_γ model.

For four cases of Hibiki et al.'s experiments, void fraction concentrated in core was well predicted as shown in Fig. 6. However, differently with the DEDALE 1101 case, the calculated bubble size S_γ model is relatively smaller than the experimental data even though their profiles follow well the tendency of the bubble size as shown in the Fig. 7. These differences in the bubble size prediction for the two data sets were believed to come from different way of air injection at inlet and the geometry of test section. However phase velocities were well predicted as in Fig. 8 and 9.

In the application of new bubble size model to the Hibiki et al.'s data, the model shows also better prediction capability that the S_γ model as in the DEDALE cases.

Finally, we can conclude that the new bubble size-correlation could be applicable to the local bubble size of not only air-water experiment in low pressure condition but also subcooled boiling experiment in high pressure condition. Fig. 10 shows the local bubble size predicted by correlation with the experimental data including DEBORA subcooled data and DEDALE and Hibiki et al.'s air-water data. It shows that present bubble size correlation predicts the local bubble size within 30% of deviation against experimental data.

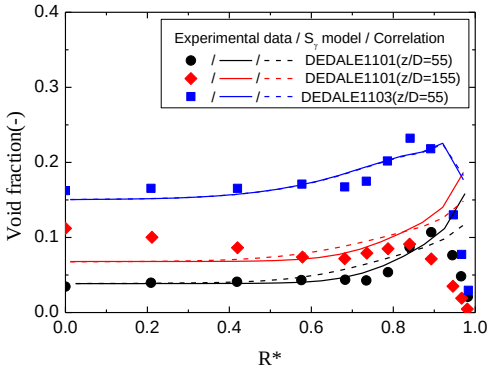

Fig. 2. Comparison of the Void Fraction Prediction with the DEDALE Experimental Data

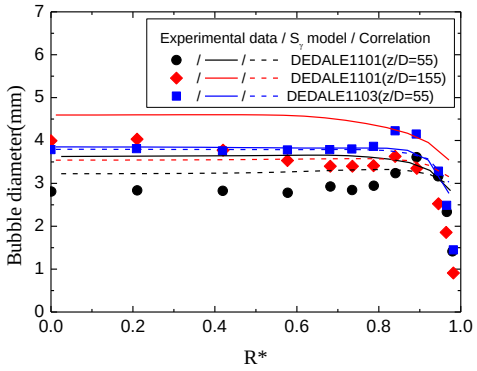

Fig. 3. Comparison of the Bubble Diameter Prediction with the DEDALE Experimental Data

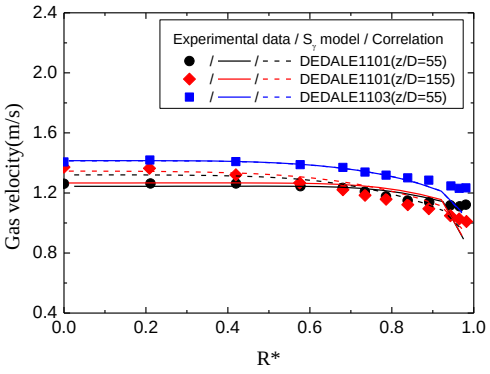

Fig. 4. Comparison of the Gas Velocity Prediction with the DEDALE Experimental Data

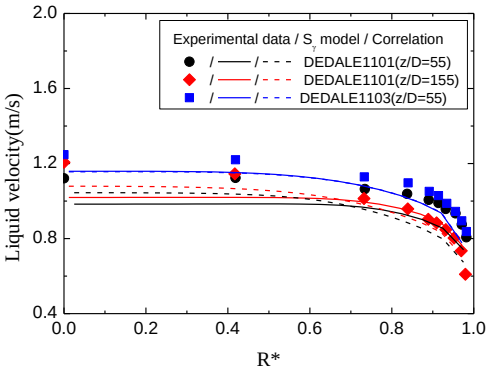

Fig. 5. Comparison of the Liquid Velocity Prediction with the DEDALE Experimental Data

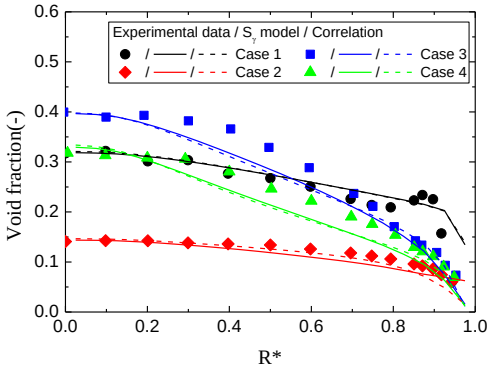

Fig. 6. Comparison of the Void Fraction Prediction with the Hibiki et al.'s Experimental Data

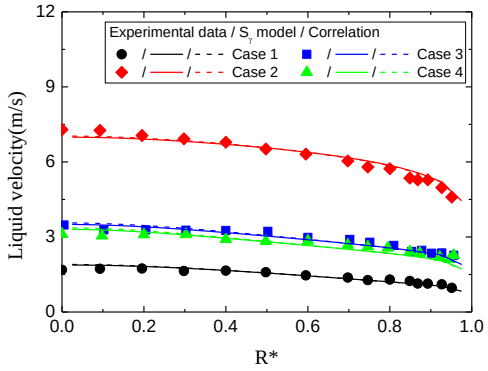

Fig. 9. Comparison of the Liquid Velocity Prediction with the Hibiki et al.'s Experimental Data

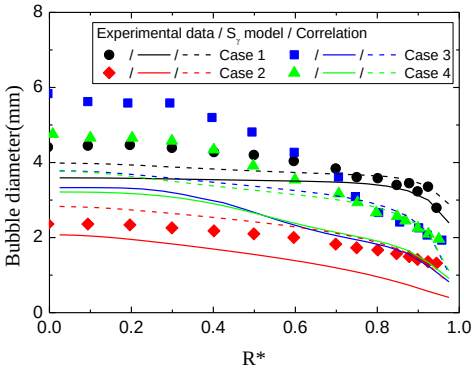

Fig. 7. Comparison of the Bubble Diameter Prediction with the Hibiki et al.'s Experimental Data

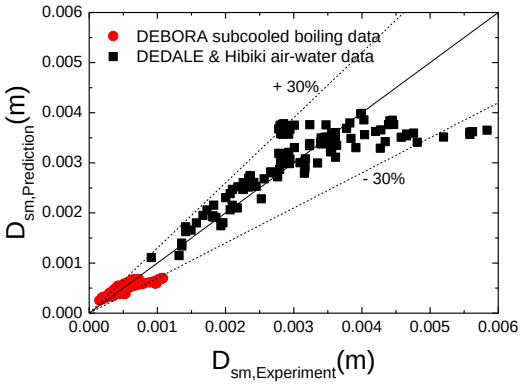

Fig. 10. Comparison of the Local Bubble Size Prediction with Experimental Data

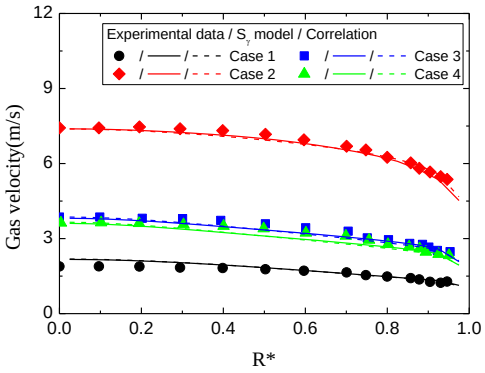

Fig. 8. Comparison of the Gas Velocity Prediction with the Hibiki et al.'s Experimental Data

6. Conclusion

In this study, Three-dimensional numerical simulations were carried out to evaluate the performance of S_γ model in air-water flow using the commercial CFD code STAR CCM$^+$ ver. 9.06. S_γ model was evaluated against DEDALE and Hibiki et al.'s air-water experimental data obtained in the vertical pipes. All numerical results predicted reasonably the two-phase flow parameters such as the void fraction, the bubble size and the phasic velocities. In the further studies, S_γ model will be applied to the prediction of boiling phenomena in the narrow rectangular channel for the research reactor.

Additionally, correlation for the prediction of local bubble size was developed on the basis of DEDALE, Hibiki et al.'s and DEBORA data. The correlation was compared against experimental data. The results indicated that present model is satisfactory for the prediction of available air-water experimental data.

ACKNOWLEDGMENTS

This work was supported by Nuclear Research & Development Program of the NRF (National Research Foundation of Korea) grant funded by the MSIP(Ministry of Science, ICT and Future Planning) and by the Nuclear Safety Research Center Program of the KORSAFe grant funded by Nuclear Safety and Security Commission (NSSC) of the Korean government (Grant code: NRF-2012M2B2A6028182, 1305011).

NOMENCLATURE

n	[m^{-3}]	Number density
M_r	[-]	Moment of size distribution
$P(d)$	[-]	Bubble size distribution
a_i	[m^{-1}]	Interfacial area density
u	[m/s]	Velocity
K_{br}	[s^{-1}]	Breakup rate
d	[m]	Bubble diameter
K_{cl}	[s^{-1}]	Coalescence rate
k_{coll}	[-]	Collision rate coefficient
P_{cl}	[-]	Coalescence probability of a single collision event
We	[-]	Weber number
L_k	[m]	Kolmogorov length scale
C_α	[-]	Dispersed concentration factor
d_{eq}	[m]	Equivalent mean diameter
k_{br}	[s]	Inertia breakup time
t_i	[s]	Interaction time
t_d	[s]	Film drainage time
F_i	[N]	Interaction force
h_{cr}	[m]	Critical film thickness
g	[m/s^{-2}]	Acceleration of gravity

Special characters

α	[-]	Void fraction
τ_{br}	[s]	Breakup time
Ω	[-]	Capillary number
ε	[m^2/s^3]	Continuous phase dissipation rate of turbulent kinetic energy
σ	[N/m]	Surface tension
μ	[Pa· s]	Dynamic viscosity
ρ	[kg/m^3]	Density
$\dot{\gamma}$	[s^{-1}]	Shear rate

Subscripts

br	Breakup
cl	Coalescence
cr	Critical
c	Continuous phase
d	Dispersed phase
max	Maximum

REFERENCES

[1] Yao W. and Morel C., Volumetric interfacial area prediction in upward bubbly two-phase flow, International Journal of Heat and Mass Transfer, Vol. 47, No. 2, p. 307, 2004.
[2] Yeoh G. H., and Tu J. Y., A unified model considering force balances for departing vapour bubbles and population balance in subcooled boiling flow, Nuclear Engineering and Design, Vol. 235, No. 10, p. 1251, 2005.
[3] Lo S. and Zhang D.H., Modelling of break-up and coalescence in bubbly two-phase flows, The Journal of Computational Multiphase Flows, Vol. 1, No. 1, p. 23, 2009.
[4] Hibiki T., Ishii M., and Xiao Z., Axial interfacial area transport of vertical bubbly flows, International Journal of Heat and Mass Transfer, Vol. 44, No.10, p. 1869, 2001.
[5]Yun B. J., Development of advanced analysis technology for the core-catcher component against severe accident, Final Report (2012M5A4A1047940), Pusan national univ,. 2013.
[6] Yun, B. J., Splawski, A., Lo, S., and Song, C. H., Prediction of a subcooled boiling flow with advanced two-phase flow models, Nuclear engineering and design, Vol. 253, p. 351, Dec. 2012.
[7] Troshko A. A. and Hassan Y. A., A two-equation turbulence model of turbulent bubbly flows, International Journal of Multiphase Flow, Vol. 27, No. 11, 2001, pp. 1965-2000.
[8] Antal S.P., Lahey Jr. R.T., Flaherty J.E., Analysis of phase distribution in fully developed laminar bubbly two-phase flow, International Journal of Multiphase Flow, Vol. 17, No. 5, p. 635, 1991.
[9] Bozzano G. and Dente M., Shape and terminal velocity of single bubble motion: a novel approach, Computer and Chemical Engineering, Vol. 25, No. 4, p. 571, 2001.